Int. J. Electrochem. Sci., 16 **(2021)** Article ID: 21077, doi: 10.20964/2021.07.30

International Journal of
ELECTROCHEMICAL
SCIENCE
www.electrochemsci.org

A Novel Prior Noise Correction - Adaptive Extended Kalman Filtering Method for the Full Parameter and State-of-energy co-estimation of the Lithium-ion Batteries

Lili Xia, Shunli Wang, Chunmei Yu, Cong Jiang, Yongcun Fan, Wen Cao*

School of Information Engineering, Southwest University of Science and Technology, Mianyang 621010, China;
*E-mail: 497420789@qq.com

Received: 28 February 2021 / *Accepted:* 9 April 2021 / *Published:* 31 May 2021

In the battery management system, the state-of-energy is an important state to represent the remaining energy of the battery. The equivalent circuit model is the key to predicate this state of the lithium-ion battery. Therefore, the modeling and parameter identification of the battery model is crucial. This paper proposes a full parameter identification algorithm based on the forgetting factor recursive extended least-square algorithm, which is leveraged to calculate parameters including the open-circuit voltage of the equivalent circuit model. Besides, the prior noise correction adaptive extended Kalman filtering algorithm is derived to predict the state-of-energy with the proposed full parameters identification algorithm. The prior noise correction is an efficient method to reduce the estimation error of the extended Kalman filtering algorithm, which predicts the noise at the next moment by current noise. Comparing with the extended Kalman filtering algorithm, the noise of prior noise correction adaptive extended Kalman filtering algorithm can be corrected efficiently. In this way, the maximum error of the forgetting factor recursive extended least-square algorithm to estimate open-circuit-voltage is 0.41% under different complex working conditions comparing with actual values. The modeling accuracy by full parameters identification is higher than 99.31%. For verification of state-of-energy, two different complexes working conditions are conducted to calculated state-of-energy, the error of state-of-energy estimation is less than 1.49%. The results demonstrate that the proposed algorithm can perfect the state estimation.

Keywords: lithium-ion battery; state-of-energy; adaptive extended Kalman filtering; battery management system; parameter identification;

1. INTRODUCTION

Now, most Electric Vehicles (EVs) and Hybrid Electric Vehicles (HEVs) are powered by lithium-ion batteries [1, 2]. Compared with other types of power batteries, lithium-ion batteries have the advantages of high energy ratio, high single battery voltage, low self-discharging rate, long charge and discharge life, and no pollution, which occupy a very important position in the field of new energy sources [3-5]. In the use of lithium-ion batteries, the detection and control of lithium-ion batteries are important [6]. The accuracy of lithium-ion batteries parameter detection is related to the efficiency and safety of lithium-ion batteries.

The battery management system (BMS) is usually leveraged to detect, manage and diagnose the batteries. In BMS, the state-of-energy (SOE) is one of the most important parameters that characterize the remaining energy of lithium-ion batteries, and it is related to the residual driving mileages of EVs and HEVs [4, 7]. The accurate estimation of SOE is a guarantee for the safety of lithium-ion batteries and avoids the over-discharge and over-charge of the batteries. Besides, its accuracy can also avoid safety problems caused by sudden power failures of the EVs during driving. The SOE estimation methods can be divided into three categories [8], the first category is the model-based methods, the second category is the data-driven algorithms, and the last is the traditional methods. The model-based methods include the Kalman filtering (KF) algorithm and its improvement [4, 9, 10], particle filtering (PF) algorithm [11], and so on. The data-driven algorithms include the neural network method [12, 13], fuzzy control approach, and machine learning-based approaches [14]. The traditional methods include the integral method and open-circuit-voltage method.

Some methods developed by the neural network method and machine learning require a large number of training samples and calculations [15], which will greatly increase the computing load of the battery management system. Besides, data-driven algorithm accuracy also depends on the accuracy of the training samples. The model-based method is universal and the estimation accuracy does not depend on historical data. In the traditional method, the integral method is the basic method of SOE, but this method has accumulated errors and initial errors. The KF [9, 16] is an optimal choice to solve the problem of initial error and cumulative error in state estimation, but it is often used to estimate linear systems. Since lithium-ion batteries are non-linear systems, many improved Kalman filtering methods have been proposed to solve this problem. The widely used improved algorithm is the extended Kalman filtering (EKF) [17, 18]. The EKF approximately linearizes the nonlinear system by first-order Taylor expansion. However, the EKF can linearize the lithium-ion battery, but the Kalman filter defaults the system noise to Gaussian noise which is difficult to satisfy in practice. Therefore, KF and EKF will cause estimation errors due to system noise and measurement noise [19-21]. This paper proposes a prior noise correction adaptive extended Kalman filtering algorithm to estimate SOE.

The parameters of the equivalent circuit model (ECM) are related to accurate state prediction [22-24]. In the model-based state estimation algorithm, the open-circuit-voltage (OCV) is vital for states calculation, which is a coupling relationship of lithium-ion battery states including state-of-energy, state-of-power, and state-of-charge. At present, most studies in lithium-ion battery state prediction are estimation parameters of equivalent circuit models without OCV [25, 26]. In practical applications, it is difficult to obtain the relationship between the OCV and the state of the lithium-ion battery under various scenarios. Therefore, online estimation of OCV is essential, and it provides a method to calculate OCV that is not affected by the working conditions. In this research, the Thevenin model with noise correction is proposed as the model to study SOE estimation with online full parameters identification by forgetting factor recursive extended least-square (FFRELS) algorithm.

2. MATHEMATICAL ANALYSIS

2.1. Modeling and full parameter identification

The lithium-ion battery model reflects the working characteristics of lithium-ion batteries, and an accurate model plays an important role in the accuracy of state estimation [13, 27-30]. The equivalent model of a lithium-ion battery can be divided into the electrochemical model and equivalent-circuit model[31, 32]. The electrochemical model can better reflect the working conditions of lithium-ion batteries [33, 34], but the model is complex, which is not conducive to engineering applications. Compared with the electrochemical model [35, 36], the equivalent-circuit model can reflect the dynamic and static characteristics of the battery through a simple circuit model and has higher accuracy.

Common equivalent-circuit models include the PNGV model[37], Thevenin model [38-40], Rint model, and GNL model [41]. The Rint model is simple, but it does not consider the polarization reaction during the charging and discharging of lithium-ion batteries. The GNL model can fully reflect the polarization characteristics and self-discharge characteristics of lithium-ion batteries, but this model is complicated for parameter identification so it is not conducive to engineering applications. The PNGV model and the Thevenin model are not complicated and can also reflect the polarization reaction of lithium-ion batteries. The research by He [42] illustrated that the Thevenin model is the most accurate to reflect the characteristics of the ternary lithium-ion batteries. Besides, the Thevenin model has fewer parameters. Therefore, this paper adopts the Thevenin model with noise correction as the model to estimate SOE, which can accurately reflect the characteristics of lithium-ion batteries and reduce the influence of noise.

In the improved ECM, the ohmic internal resistance of the battery is reflected by the resistance R_0, and the polarization effect of lithium-ion batteries is simulated by RC parallel circuit, which is shown in Figure 1. In this figure, U_{OC} is the open-circuit-voltage of the lithium-ion battery, and U_L is the output voltage. R_P and C_P are used to represent the polarization characteristics.

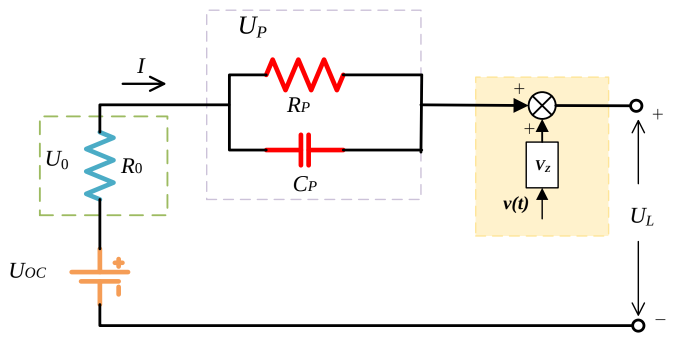

Figure 1. The improved Thevenin equivalent-circuit model

Wherein, the voltage of resistance R_0 is set as U_0 when the current is I, the voltage of the RC parallel circuit of the ECM is U_P, so Eq. (1) can be derived by the Kirchhoff voltage principle. In this paper, negative numbers of current indicate discharging and positive numbers are charging of the lithium-ion battery.

$$\begin{cases} U_L = U_{OC} - U_0 - U_P + v(t) \\ \dot{U}_P = -\dfrac{1}{R_P C_P} U_P + \dfrac{1}{C_P} I \end{cases} \quad (1)$$

In Eq. (1), the output voltage U_L and the current I in the circuit can be measured. The parameters need to be identified including open-circuit-voltage U_{OC}, ohmic internal resistance R_0, polarization resistance R_P, polarization capacitance C_P, and measurement noise represents by $v(t)$. Therefore, five parameters need to be identified.

The principle of the RELS algorithm is based on the least-square algorithm, and its implementation is mainly based on the principle of minimum mean square error. Taking the voltage of the lithium-ion battery as the output and the currents as the input, it can be regarded as a single-input-single-output (SISO) model. Therefore, Eq (1) can be obtained by Laplace transform to Eq. (2).

$$\begin{cases} U_a(s) = U_{OC}(s) - U_L(s) \\ U_a(s) = R_0 I(s) + \dfrac{R_P I(s)}{1+\tau s} + v(s) \end{cases} \quad (2)$$

Wherein, τ represents the time-constant of the RC parallel circuit. Then, the discrete system as shown in the following equation can be obtained with bilinear transformation, which is shown as follows Eq. (3).

$$\begin{cases} y(k) = y_{OCV}(k) - y_L(k) \\ y(k) = -ay(k-1) + bu(k) + cu(k-1) + n_1 v(k) + n_2 v(k-1) \\ y_L(k) = y_{OCV}(k) + ay_{OCV}(k-1) - ay_L(k-1) - bI(k) - cI(k-1) - n_1 v(k) - n_2 v(k-1) \end{cases} \quad (3)$$

In the above equations, the $y_L(k)$ represents terminal voltage, $y_{OCV}(k)$ is the OCV in the ECM. The variables a, b and c are leveraged to represent the coefficients in Eq. (3). Wherein, the coefficients of the discrete system are shown in Eq. (4).

$$\begin{cases} a = \dfrac{T - 2\tau}{T + 2\tau} \\ b = \dfrac{TR_P + TR_0 + 2R_0\tau}{T + 2\tau} \\ c = \dfrac{TR_P + TR_0 - 2R_0\tau}{T + 2\tau} \end{cases} \quad (4)$$

According to the lithium-ion battery system in Eq. (3). The output $y_L(k)$ can be reinterpreted as the least-square expression. It is crucial to OCV online identification, so $y_{OCV}(k)$- $ay_{OCV}(k$-1) combine with the coefficients are regarded as the identification variables. The system can be rewritten as Eq. (5).

$$\begin{cases} y_L(k) = x(k)^T \cdot \theta \\ x(k) = \begin{bmatrix} 1 & y_{UL}(k-1) & I(k) & I(k-1) & v(k) & v(k-1) \end{bmatrix}^T \\ \theta = \begin{bmatrix} y_{OCV}(k) + ay_{OCV}(k-1) & -a & -b & -c & -n_1 & -n_2 \end{bmatrix}^T \end{cases} \quad (5)$$

In the RELS algorithm, the noise has seemed as the variable of lithium-ion, and the influence of noise is taken into account, which improves the accuracy of parameter estimation. In Eq. (5), the $v(k)$ is the noise in the battery system, and n_1 and n_2 are the related parameters. According to the recursive extended least-square algorithm, which is shown as Eq. (6), the parameters can be calculated by the RELS estimation results and the coefficients which are shown in Eq. (4).

$$\begin{cases} \theta(k) = \theta(k-1) + \gamma \cdot P(k-1)x(k)[y_L(k) - x^T(k)\theta(k-1)] \\ \gamma = \left[x^T(k)P(k-1)x(k) + \lambda\right]^{-1} \\ P(k) = [I - \gamma \cdot P(k-1)x(k)x^T(k)]P(k-1)/\lambda \end{cases} \quad (6)$$

In the above equation, λ is the forgetting factor, which can reduce the influence of old data. The *P*(*k*) denotes the error covariance matrix. To acquire high accuracy parameter identification results, the initial values of *θ*(*k*) should set as small as possible, *P*(*k*) is supposed to set as an identity matrix with great gain.

2.2. Prior noise correction-adaptive extended Kalman filtering

The state-of-energy, which represents the remaining energy of the battery, is a vital parameter of BMS. It reflects the current energy of lithium-ion batteries so that it can better reflect the endurance mileage when the lithium-ion batteries are used as the power of electric vehicles. Its definition is shown in Eq (7).

$$SOE(k) = SOE(0) - \frac{\int_0^k \eta I(k) U_L(k) dk}{E_0} \quad (7)$$

Wherein, the E_0 is the initial value of lithium-ion batteries, *SOE*(0) is the SOE at the initial moment, η is the Coulomb efficiency, *I*(*k*) and $U_L(k)$ are the output current and voltage, respectively, which can be measured by sensors. According to equation (7), by selecting appropriate input and output, the state space equation of the equivalent circuit model can be obtained. The calculation of SOE [43, 44] and the output equation of the lithium-ion battery system are shown in Eq. (8).

$$\begin{cases} \begin{bmatrix} SOE(k) \\ U_{P,}(k) \end{bmatrix} = \begin{bmatrix} 1 & 0 \\ 0 & e^{-\frac{T}{\tau}} \end{bmatrix} \begin{bmatrix} SOE(k-1) \\ U_P(k-1) \end{bmatrix} + \begin{bmatrix} -\dfrac{\eta \Delta k U_L(k)}{E_0} \\ R_P(1-e^{-\frac{T}{\tau}}) \end{bmatrix} I(k) + \omega(k) \\ U_L(k) = Uoc(k) + \begin{bmatrix} 0 \\ 1 \end{bmatrix}^T \begin{bmatrix} SOE(k) \\ U_P(k) \end{bmatrix} + R_0 I(k) + v(k) \end{cases} \quad (8)$$

Wherein, the $\omega(k)$ in equation (8) is the system noise matrix, $\omega(k) = \left[\omega_1(k) \quad \omega_2(k)\right]^T$. The $v(k)$ in this equation is the measurement error matrix.

Kalman filtering is one of the optimal filtering methods. At first, this method predicts the state at times *k*, then it calculates the compensation gain and the system residual to correct the predicted value, thus the final state prediction results can obtain. This method can accurately calculate the state of the system, but it does not apply to estimation errors caused by nonlinear systems and colored noise. In this research, an improved prior noise correction adaptive extended Kalman filtering (PNC-AEKF) was proposed to estimate SOE. Since it is difficult to meet the requirements of the extended Kalman filtering algorithm for noise in practical applications, estimation errors will be caused. The prior noise correction method can realize adaptive noise correction and reduce prediction errors. The extended Kalman filter algorithm uses the first-order Taylor expansion to linearize the nonlinear system. Therefore, a nonlinear system can be represented by Eq. (9).

$$\begin{cases} x_{k+1/k} = f(x_k, u_k) + \frac{\partial f(x_k, u_k)}{\partial x_k}\Big|_{x_k = x_{k+1/k}} (x_k - x_{k+1/k}) + \omega_k \\ y_k = g(x_k, u_k) + \frac{\partial g(x_k, u_k)}{\partial x_k}\Big|_{x_k = x_{k+1/k}} (x_k - x_{k+1/k}) + v_k \end{cases} \tag{9}$$

For the SOE estimation, step 1 is calculating the state prediction and estimate the error covariance matrix.

$$\begin{cases} x_{k+1/k} = Ax_k + Bu_{k+1} + \omega_{k+1} \\ P_{k+1/k} = AP_k A^T + Q_k \end{cases} \tag{10}$$

Wherein x_k is the state vector, A is the state transition matrix, B is the control matrix. In this formula, $P_{k+1/k}$ is the predicted error covariance matrix, Q_k is the noise covariance matrix which generates by the lithium-ion battery system. Step 2 is calculating the Kalman gain.

$$K_{k+1} = P_{k+1/k} C^T (CP_{k+1/k} C^T + R_k)^{-1} \tag{11}$$

In equation (11), C is the measurement matrix of the system. R_k is measurement noise. Step 3 is predicting the state at the next moment and updating the error covariance matrix at the next moment.

$$\begin{cases} \zeta_{k+1} = y_{k+1} - (Cx_{k+1/k} + Du_{k+1}) \\ x_{k+1} = x_{k+1/k} + K_{k+1}\zeta_{k+1} \\ P_{k+1} = (E - K_{k+1}C)P_{k+1/k} \end{cases} \tag{12}$$

Wherein, ζ_{k+1} is the system residual error, D is the feedforward matrix. SOE can be revised by ζ_{k+1}. The system noise of this algorithm has seemed as Gaussian white noise when using EKF, which ignores the noise characteristics so that the estimation error will be caused by noises in the practical application of it.

To solve errors caused by noise, this paper leverages prior noise correction to update the noise variables Q_k and R_k in the EKF algorithm. The error covariance matrix Q_k and R_k are determined by system noise and observation noise, respectively. According to their definition, the calculation equations are shown as follows.

$$\begin{cases} E\left\{\omega_k \cdot \omega_k^T\right\} = Q_k \\ E\left\{v_k \cdot v_k^T\right\} = R_k \end{cases} \tag{13}$$

Wherein, the variable ω_k is system noise, and v_k is the measurement noise. Thence, these two variables can be applied to compute the covariance matrix Q_k and R_k respectively. When the estimation result at time k+1 is obtained, the prediction equation can be used to calculate the system noise.

$$\begin{cases} \omega_{k+1} = x_{k+1} - x_{k+1/k} \\ x_{k+1} = x_{k+1/k} + K_{k+1}\zeta_{k+1} \\ K_{k+1}\zeta_{k+1} = x_{k+1} - x_{k+1/k} \\ \omega_{k+1} = K_{k+1}\zeta_{k+1} \\ Q_{k+1} = E\left\{\omega_{k+1} \cdot \omega_{k+1}^T\right\} = K_{k+1}\zeta_{k+1}\zeta_{k+1}^T K_{k+1}^T \end{cases} \tag{14}$$

According to the observation equation and the measured voltage, the observation error can be calculated, which is caused by observation noise.

$$\begin{cases} y_{k+1} = Cx_{k+1} + Du_{k+1} + v_{k+1} \\ v_{k+1} = \varepsilon_{k+1} = y_{k+1} - Cx_{k+1} - Du_{k+1} \\ R_{k+1} = E\left\{v_{k+1} \cdot v_{k+1}^T\right\} = \varepsilon_{k+1} \cdot \varepsilon_{k+1}^T \end{cases} \tag{15}$$

Wherein, the variable ε_{k+1} represents the residual in the battery system. To consider the impact of sudden changes in noise, a forgetting factor is increased to improve the stability of the estimation results. The adaptive equation is shown below.

$$\begin{cases} Q_{k+1} = (1-d_k)Q_k + d_{k+1}\left(K_k \zeta_{k+1} \zeta_{k+1}^T K_k^T\right) \\ \zeta_{k+1} = y_{k+1} - Cx_{k+1/k} - Du_{k+1} \\ R_{k+1} = (1-d_k)R_k + d_{k+1}\left(\varepsilon_{k+1} \cdot \varepsilon_{k+1}^T\right) \\ \varepsilon_{k+1} = y_{k+1} - Cx_{k+1} - Du_{k+1} \end{cases} \tag{16}$$

In Eq (16), y_{k+1} is the state observation. In the next moment for SOE prediction, the covariance matrix Q_k and R_k which are estimated by prior noise correction can be adopted into the EKF algorithm. The prediction principle of SOE based on full parameter identification and PNC-AEKF algorithm is shown in Fig 2.

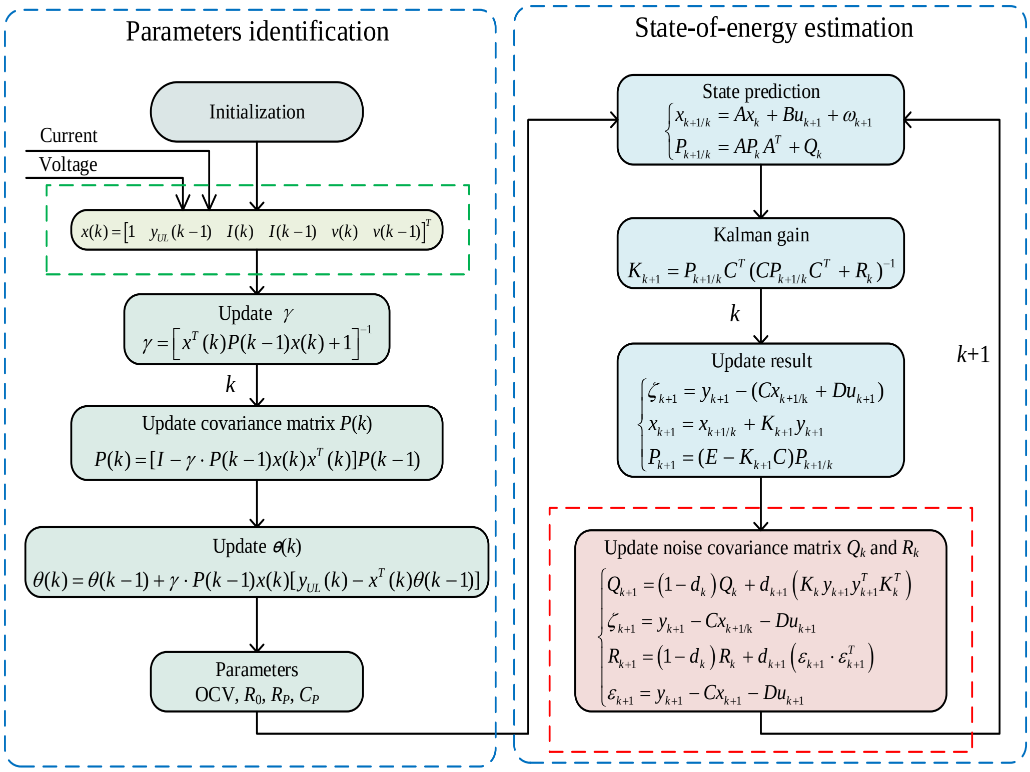

Figure 2. Prediction principle of state-of-energy

3. EXPERIMENTAL ANALYSIS

3.1. The verification of parameters identification

For verification of the parameter identification results of the ECM, 72Ah ternary lithium-ion battery was selected for experiments. For parameter identification result accuracy verification, the Beijing bus dynamic stress test (BBDST) working conditions and the dynamic stress test (DST) working conditions [45] were leveraged to identify the parameter identification results. Wherein, the BBDST and the DST are complex working conditions, both of them have come from actual automobile road tests. In this paper, the lithium-ion battery data is obtained by experiments in the laboratory. Besides, both of them were conducted at 25°C. The working steps of two working conditions are shown in Tables 1 and 2.

Table 1. The working steps of the Beijing bus dynamic stress test

steps	P/KW	t/s	condition	steps	P/KW	t/s	condition
1	45	21	starting	11	12	16	glissade
2	80	12	speed up	12	-15	6	breaking
3	12	16	glissade	13	80	9	speed up
4	-15	6	braking	14	100	6	rapidly
5	45	21	speed up	15	45	21	constant
6	12	16	glissade	16	12	16	glissade
7	-15	6	braking	17	-35	9	braking
8	80	9	speed up	18	-15	12	braking
9	100	6	rapidly	19	12	71	stop
10	45	21	constant				

The BBDST working condition mainly uses the power values in each step to represent the conditions. In actually using, the power of each step was reduced in proportion. The total test time of this test is 300 seconds. In this paper, the battery is used to test by BBDST working condition circularly until reaching cut-off voltage.

Table 2. The working steps of the dynamic stress test

steps	t/s	Maximum power percentage	steps	t/s	Maximum power percentage
1	16	0%	14	36	-13%
2	28	-13%	15	2	-100%
3	12	-25%	16	6	-50%
4	8	13%	17	24	-63%
5	16	-2%	18	8	25%
6	24	-13%	19	32	-25%
7	12	-25%	20	8	50%
8	8	13%	21	12	-2%
9	16	-2%	22	2	-121%
10	24	-13%	23	5	-2%
11	12	-25%	24	2	66%
12	8	25%	25	23	-2%
13	16	-2%			

The DST working condition mainly uses the maximum power ratio to express the working conditions. The working time of each is 360 seconds of each circulation. The test method of a lithium-ion battery of DST working condition also is the same as BBDST working condition.

In the two tables above, the negative sign represents discharging of the lithium-ion battery, and the positive numbers are the charging sections. Under the BBDST working condition, the verified results of parameters identification of the improved Thevenin model are shown in Fig 3. The results of the DST working condition are shown in Fig 4.

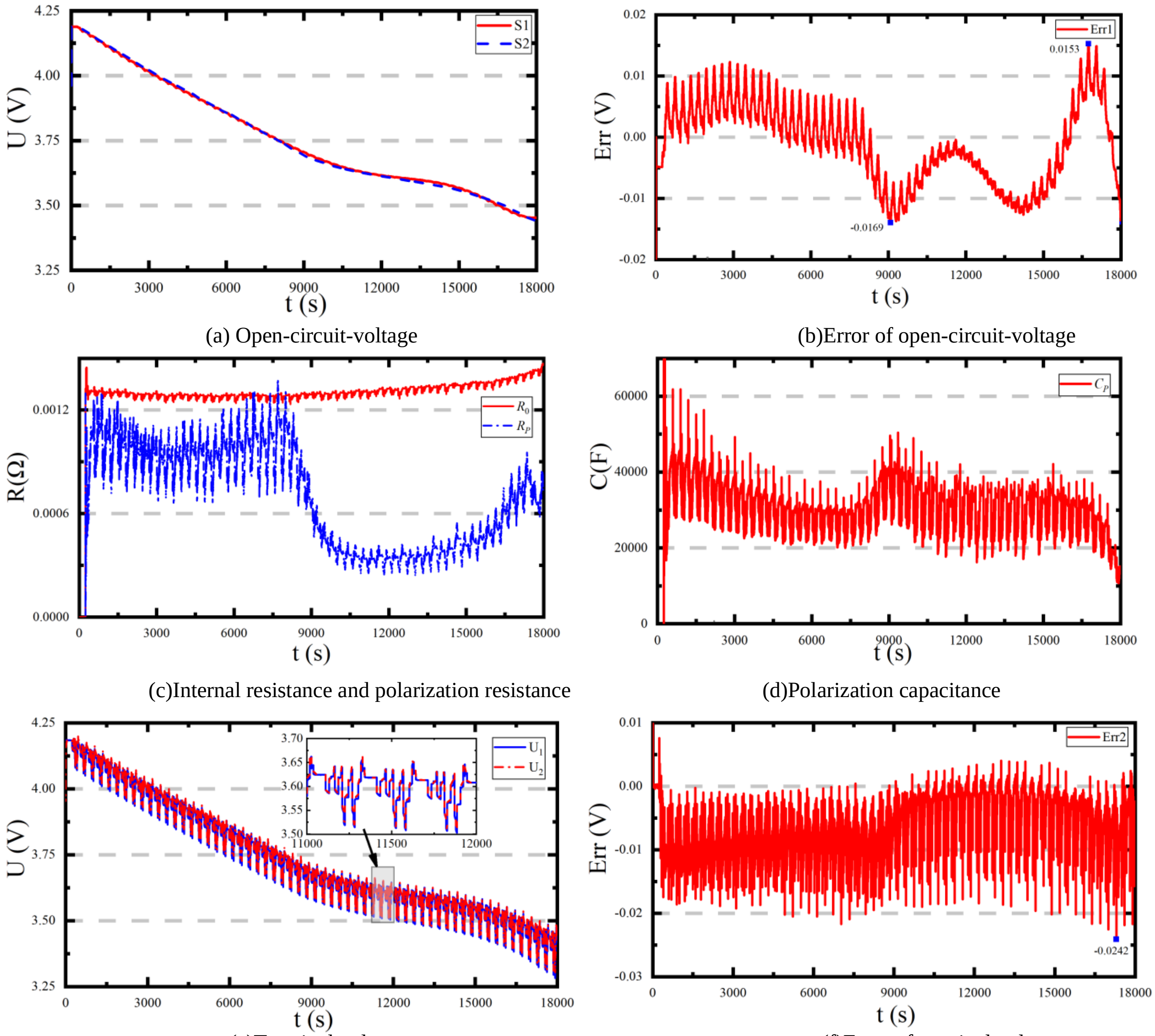

(a) Open-circuit-voltage (b)Error of open-circuit-voltage

(c)Internal resistance and polarization resistance (d)Polarization capacitance

(e)Terminal voltage (f)Error of terminal voltage

Figure 3. Parameters identification base on Beijing bus dynamic stress test working condition

Figure 3(a) is the comparison between the actual open-circuit-voltage curve and the estimated open-circuit-voltage curve which is predicted by the online full parameters identification algorithm. Wherein, S1 is the true value, and S2 is the estimated curve. Figure 3(b) is the online OCV estimation error. The maximum value of the error is 16.9 mV, which is less than 0.41%, indicating that the prediction result is reliable. Figure 3(c) and (d) are the remaining parameters in the proposed ECM. Due to internal chemical reaction, the internal resistance, polarization resistance and polarization capacitance of the battery will change with the charge and discharge rate. Therefore, the fluctuation of the parameters is mainly caused by the charge and discharge rates. Figure 3(e) is the simulation voltage by the identified parameters and the measured terminal voltage by the sensor. Wherein, U_1 is the simulation value and the U_2 is the measured. The error between the simulation voltage and the actual value is shown in figure 3(f). Wherein, the maximum error is 24.2 mV, which is less than 0.58%. This result can conclude that this ECM has high precision and parameter identification result is efficient. By comparing with the modeling accuracy in references [39], [40], and [41], the proposed model can better characterize the working characteristics of the battery than the references.

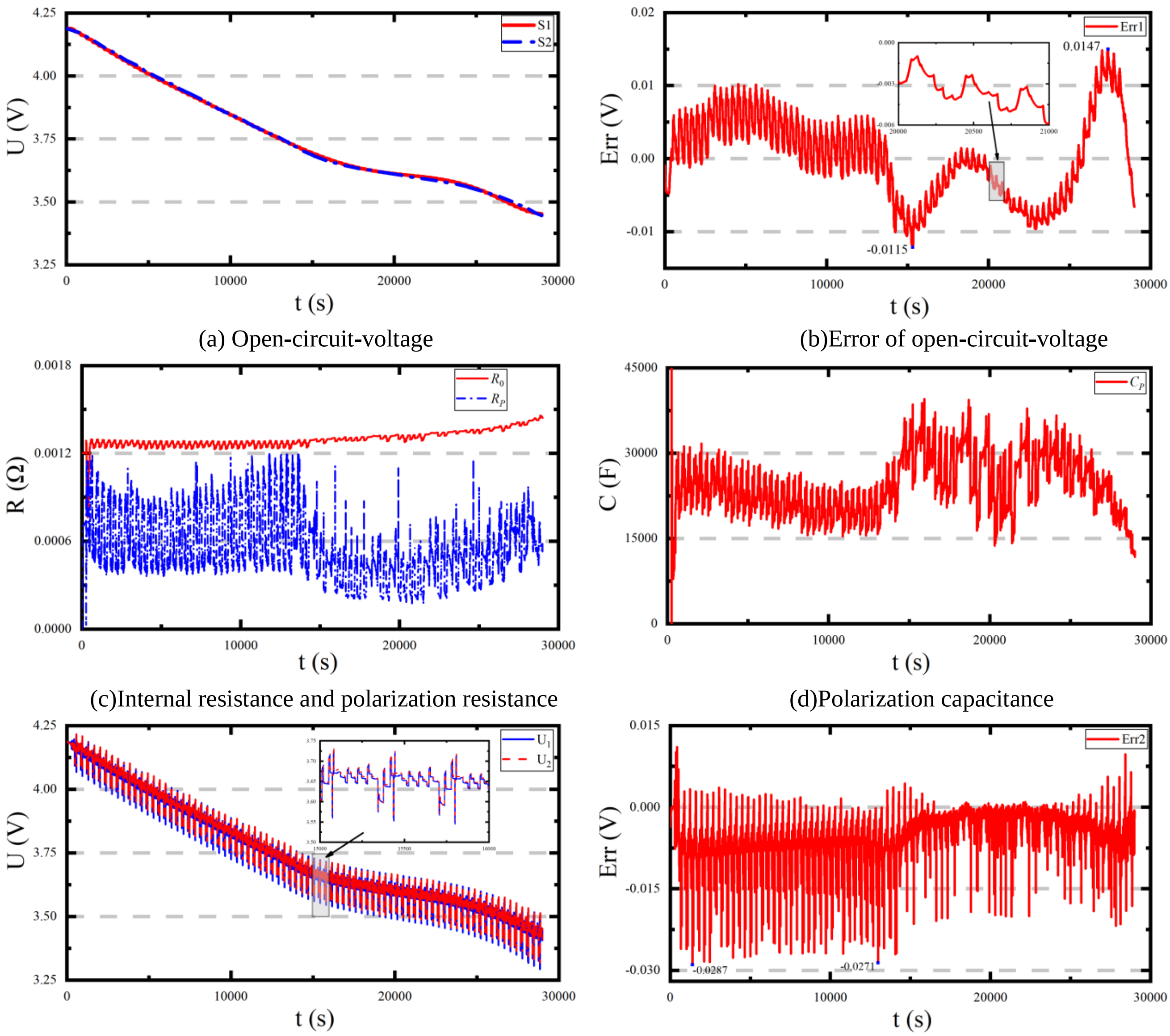

(a) Open-circuit-voltage

(b)Error of open-circuit-voltage

(c)Internal resistance and polarization resistance

(d)Polarization capacitance

(e)Terminal voltage

(f)Error of terminal voltage

Figure 4. Parameters identification base on dynamic stress test working condition

The above figures are the simulation result of parameters identification results verification under DST working conditions. In figure 5(a), the simulation result S2 is the estimated OCV. It can conclude that the OCV prediction is accurate from figure 4(b). The maximum error is 14.7 mV, which is less than 0.35%. The parameters identification verification is the figure 4(e) and (f). The curve U_1 is the real voltage of the lithium-ion battery, U_2 is the simulation result to verify the accuracy of identified parameters. From figure 4(f), the error is no more than 28.7mV, the maximum value is 0.69%.

3.2. State of energy estimation under Beijing bus dynamic stress test working condition

About SOE estimation, MATLAB was used for simulation, and the parameters of the equivalent circuit model identified by the full parameter identification algorithm are taken into the SOE estimation. EKF algorithm and PNC-AEKF algorithm were used to estimate the SOE under the BBDST experiment. Figure 5(a) shows the comparison between simulation results of SOE estimation of lithium-ion battery by two different algorithms and real SOE. Figures 5(b) and 5(c) are the enlarged view of SOE estimation results. Figure 5(d) shows the error curves of SOE estimation by two algorithms under BBDST.

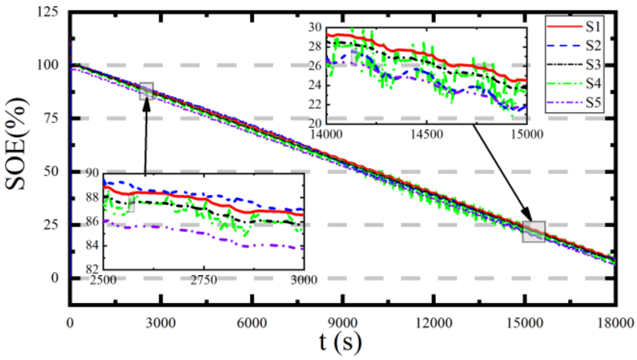

(a) State-of-energy estimation

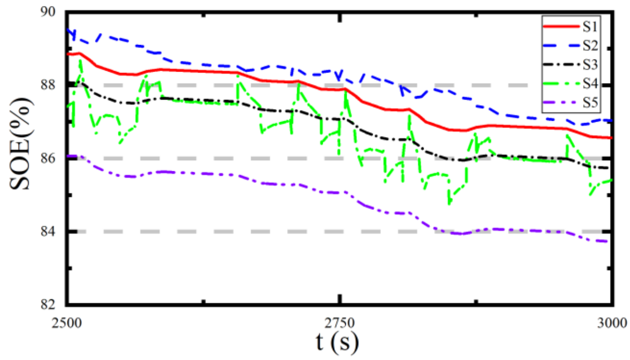

(b)Enlarged view of state-of-energy estimation

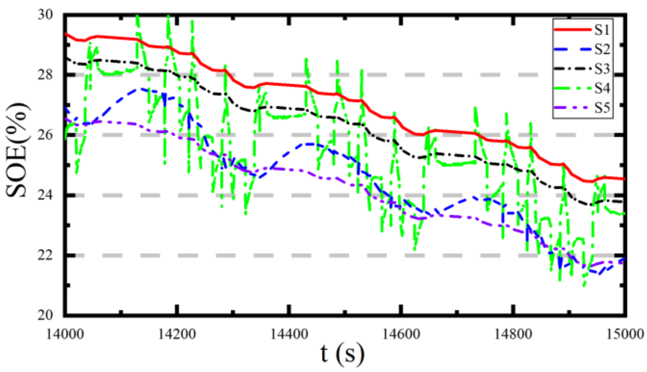

(c)Enlarged view of state-of-energy estimation

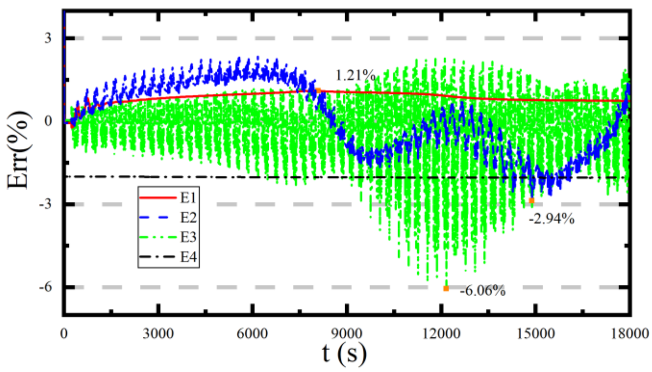

(d)State-of-energy estimation error

Figure 5. State-of-energy estimation results under Beijing bus dynamic stress test working condition

In figure 6(a), the S3 is the real SOE, S1, S2, S4, and S5 are the SOE estimated by the improved AEKF algorithm, EKF algorithm, BP neural network, and integral method respectively. Among them, the initial SOE value of the integral method, EKF, and improved AEKF is set to 98%, and the actual initial value of SOE is 100%. From the enlarged figures can conclude that the prior noise correction can enhance the tracking performance of the EKF algorithm. It is easy to find that the improved method can effectively reduce the fluctuation of SOE estimation. Besides, the simulation results show that the proposed AEKF can reduce the initial error compare with the integral method. The S4 is the experimental result from the BP algorithm, and the neural network model is trained by DST working conditions. Compared with the AEKF, it can conclude that the AEKF has better versatility than BP neural network algorithm. In figure 6(d), E1 is the PNC-AEKF estimation error, and E2 is the EKF estimation error. In BBDST working conditions, the maximum error is 1.21% by the PNC-AEKF algorithm, the maximum error is 2.94% of EKF. E3 and E4 are the errors of BP and integral methods respectively. The simulation results show that the proposed improved method can enhance the robustness of SOE estimation and improve the accuracy and has better performance than other SOE estimation methods. In reference [43] and [44], the SOE estimation results are obtained by improved EKF. In both of them, the error is exceeded 4%. Compared with the methods proposed in reference [43] by Lin and reference [44] by Li, the method in this paper can better estimate the SOE and the error is significantly smaller than the references.

During the discharge of lithium batteries, since the EKF algorithm ignores the characteristics of noise in the discharge process, the accumulated noise error will gradually diverge SOE estimation error. The error variation in the EKF algorithm in figure 5(d) can be verified well. At the same time, with the further decrease of SOE of the lithium-ion battery, the nonlinear degree of the lithium-ion battery will be more intense. The EKF algorithm will further increase the estimation error because it ignores the higher-order term of the system.

By comparing the simulation results of the improved algorithm and EKF algorithm, the advantages of adding adaptive prior noise correction for noise correction to SOE estimation are illustrated. This method can effectively improve the accuracy of SOE estimation and make up for the shortcoming that the EKF algorithm does not consider noise characteristics.

3.3. State of energy estimation under dynamic stress test working condition

The dynamic stress test is a kind of complicated working condition simplified by the working condition of the federal city in the United States, which plays an important role in verifying the estimation of SOE by an algorithm. In this paper, DST working conditions also was adopted to verify this algorithm. The estimation result of the PNC-AEKF algorithm about SOE under DST condition is shown in figure 6.

In figure 6(a), S1, S2, S3, S4, and S5 are the PNC-AEKF estimation results, EKF estimation result, real value, BP neural network prediction results, and integral method estimated SOE respectively. The SOE estimation result by the improved algorithm in DST working conditions is closest to the real SOE value than the other algorithms, which is consistent with the result obtained under BBDST working conditions. In figure 6(d), E1 is the error of the PNC-AEKF algorithm, whose maximum error is 1.49%, and E2 is the error of the EKF algorithm, whose maximum error is 2.16%. E3 is the estimation error of the BP algorithm, and the model is trained by BBDST working conditions, the error shows that the generalization is poor of the neural network to estimate SOE than AEKF. E4 is the simulation error of the integral method, the error proves that the proposed AEKF can make up the shortcoming of the integral method. The comparison results of the two algorithms also show that adaptive filtering can effectively solve the error accumulation caused by noise and improve the accuracy of SOE estimation. Besides, the simulation results also batter than the references [43] and [44] of SOE estimation.

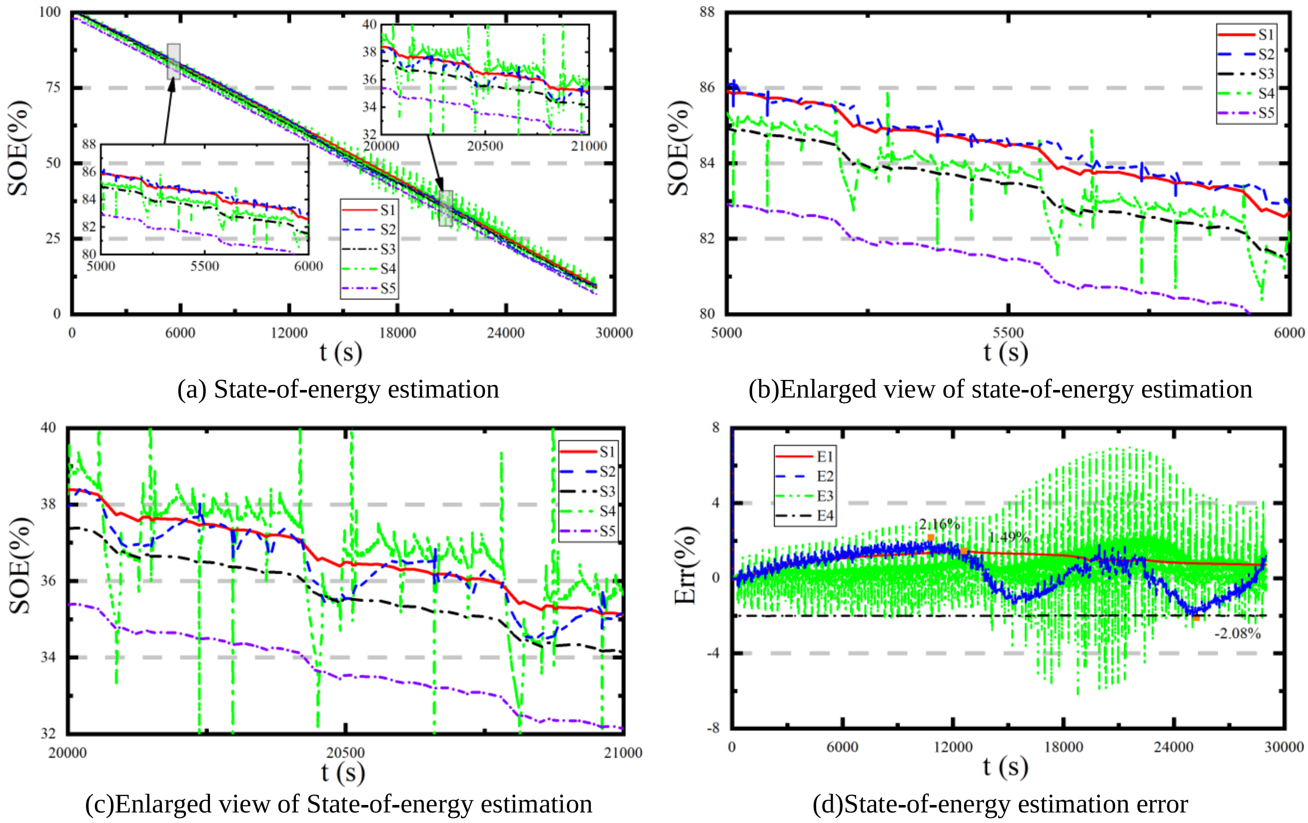

Figure 6. State-of-energy estimation results under dynamic stress test working condition

4. CONCLUSIONS

In this paper, the improved Thevenin model was adopted as the equivalent circuit model of the lithium-ion battery. For full parameters online identification, the FFRELS algorithm is leverage to estimate parameters with the proposed least-square expression method. The experimental results show that this method can identify parameters effectively, the maximum voltage error is no exceed 28.7 mV under complex conditions. Besides, the improved PNC-AEKF algorithm is adopted to estimate SOE under different working conditions. Compared with the other algorithms, the simulation results show that the proposed algorithm with adaptive prior noise correction is more accurate than the traditional EKF algorithm and other methods, the improved algorithm avoids the cumulative error caused by the

EKF algorithm ignoring noise characteristics. The simulation results show that the noise accumulation error in the EKF algorithm can be reduced by prior noise correction, and the improved PNC-AEKF algorithm enhances the accuracy of SOE estimation of lithium-ion battery and the robustness is better than the EKF algorithm and the generalization is good of proposed algorithm.

ACKNOWLEDGMENTS
The work was supported by the National Natural Science Foundation of China (No. 61801407).

References

1. P. Iurilli, C. Brivio and M. Merlo, *Sustainable Energy, Grids and Networks*, 19 (2019) 100230.
2. P. Shrivastava, T. K. Soon, M. Y. I. B. Idris and S. Mekhilef, *Renewable and Sustainable Energy Reviews*, 113 (2019) 109233.
3. Y. Guo, Z. Zhao and L. Huang, *Energy Procedia*, 105 (2017) 4146.
4. S. Wang, D.-I. Stroe, C. Fernandez, C. Yu, C. Zou and X. Li, *Journal of Power Sources*, 450 (2020) 227652.
5. K.-H. Shin, C.-S. Jin, J.-Y. So, S.-K. Park, D.-H. Kim and S.-H. Yeon, *Journal of Energy Storage*, 27 (2020) 101066.
6. Y. Zheng, J. Wang, C. Qin, L. Lu, X. Han and M. Ouyang, *Energy*, 185 (2019) 361.
7. J. Du, X. Zhang, T. Wang, Z. Song, X. Yang, H. Wang, M. Ouyang and X. Wu, *Energy*, 165 (2018) 153.
8. G. Zhai, S. Liu, Z. Wang, W. Zhang and Z. Ma, *Energy Procedia*, 105 (2017) 3146.
9. Y. Bi and S.-Y. Choe, *Applied Energy*, 258 (2020) 113925.
10. X. Hu, H. Jiang, F. Feng and B. Liu, *Applied Energy*, 257 (2020) 114019.
11. R. Xiong, Y. Z. Zhang, H. W. He, X. Zhou and M. G. Pecht, *Ieee T Ind Electron*, 65 (2018) 1526.
12. H. Ben Sassi, F. Errahimi, N. Es-Sbai and C. Alaoui, *Journal of Energy Storage*, 25 (2019) 100822.
13. Y. C. Song, D. T. Liu, H. T. Liao and Y. Peng, *Appl Energ*, 261 (2020) 114408.
14. Z. Deng, L. Yang, Y. Cai and H. Deng, *Energy Procedia*, 107 (2017) 68.
15. Y. Guo, Z. Zhao and L. Huang, *Energy Procedia*, 105 (2017) 4153.
16. K. Zhang, P. Zhao, C. Sun, Y. Wang and Z. Chen, *Chinese Journal of Aeronautics*, 33 (2020) 1517.
17. Y. Wang, C. Zhang and Z. Chen, *Energy Procedia*, 88 (2016) 998.
18. S. Wang, C. Fernandez, L. Shang, Z. Li and J. Li, *Journal of Energy Storage*, 9 (2017) 69.
19. D. Xile, Z. Caiping and J. Jiuchun, *Energy Procedia*, 152 (2018) 520.
20. A. K. Mishra, S. R. Shimjith and A. P. Tiwari, *IFAC-PapersOnLine*, 51 (2018) 702.
21. J. Luo, J. Peng and H. He, *Energy Procedia*, 158 (2019) 3421.
22. K. Propp, D. J. Auger, A. Fotouhi, M. Marinescu, V. Knap and S. Longo, *Journal of Energy Storage*, 26 (2019) 100943.
23. D. Y. Tang, M. T. Gong, J. S. Yu and X. Li, *Microelectronics Reliability*, 114 (2020) 113832.
24. S. Lavety, R. K. Keshri and M. A. Chaudhari, *Journal of Energy Storage*, 33 (2021) 102031.
25. K. V. Singh, H. O. Bansal and D. Singh, *Journal of Energy Storage*, 27 (2020) 101124.
26. M. F. Niri, T. M. N. Bui, T. Q. Dinh, E. Hosseinzadeh, T. F. Yu and J. Marco, *Journal of Energy Storage*, 28 (2020) 101271.
27. L. Fang, J. Li and B. Peng, *Energy Procedia*, 158 (2019) 3008.
28. C. S. Chin, Z. Gao and C. Z. Zhang, *Journal of Energy Storage*, 28 (2020) 101222.
29. S. Zhou, X. Liu, Y. Hua, X. Zhou and S. Yang, *Journal of Power Sources*, 482 (2021) 228951.

30. S. Li, H. He, C. Su and P. Zhao, *Appl Energy*, 275 (2020) 115340.
31. X. Tang, Y. Wang, K. Yao, Z. He and F. Gao, *Journal of Power Sources*, 440 (2019) 227141.
32. M.-K. Tran, A. Mevawala, S. Panchal, K. Raahemifar, M. Fowler and R. Fraser, *Journal of Energy Storage*, 32 (2020) 101785.
33. M. Kim, H. Chun, J. Kim, K. Kim, J. Yu, T. Kim and S. Han, *Appl Energ*, 254 (2019) 113644.
34. P. M. Munoz, R. M. Humana, T. Falaguerra and G. Correa, *Journal of Energy Storage*, 32 (2020) 101803.
35. J. F. Li, D. F. Wang and M. Pecht, *Journal of Power Sources*, 436 (2019) 226885.
36. X. Lai, L. He, S. Y. Wang, L. Zhou, Y. F. Zhang, T. Sun and Y. J. Zheng, *Journal of Cleaner Production*, 255 (2020) 120203.
37. S. Castano-Solis, D. Serrano-Jimenez, J. Fraile-Ardanuy and J. Sanz-Feito, *Electric Power Systems Research*, 166 (2019) 9.
38. I. Jarraya, F. Masmoudi, M. H. Chabchoub and H. Trabelsi, *Journal of Energy Storage*, 26 (2019) 100946.
39. J. K. Peng, J. Y. Luo, H. W. He and B. Lu, *Appl Energ*, 253 (2019) 113520.
40. P. Schroer, E. Khoshbakht, T. Nemeth, M. Kuipers, H. Zappen and D. U. Sauer, *Journal of Energy Storage*, 32 (2020) 101966.
41. X. F. Ding, D. H. Zhang, J. W. Cheng, B. B. Wang and P. C. K. Luk, *Appl Energy*, 254 (2019) 113615.
42. H. W. He, R. Xiong and J. X. Fan, *Energies*, 4 (2011) 582.
43. C. Lin, H. Mu, R. Xiong and J. Y. Cao, *Appl Energy*, 194 (2017) 560.
44. X. Y. Li, K. Pan, G. D. Fan, R. G. Lu, C. B. Zhu, G. Rizzoni and M. Canova, *Journal of Power Sources*, 367 (2017) 202.
45. S. L. Wang, C. Fernandez, C. M. Yu, Y. C. Fan, W. Cao and D. I. Stroe, *Journal of Power Sources*, 471 (2020) 228450.